An *in situ operando* MEMS platform for characterization of Li-ion battery electrodes

H Jung[1,2], K Gerasopoulos[2], X Zhang[1] and R Ghodssi[1,2]*

[1] Department of Electrical and Computer Engineering, University of Maryland, College Park, MD 20742, USA

[2] Institute for Systems Research, University of Maryland, College Park, MD 20742, USA

*E-mail: ghodssi@umd.edu

Abstract. This paper presents an *in situ operando* approach that allows characterization of lithium-ion battery electrodes. A MEMS sensor is designed and integrated with a commercially available Raman spectroscope to enable monitoring the stress and structural changes in the electrodes. An interferometric method with an enhanced image processing algorithm is applied for analyzing the crystal phase-dependent stress changes – contributing to higher sensitivity compared to a previously reported technique – while the structural changes are monitored using Raman spectroscopy. New capabilities of our platform are highlighted, allowing visual observation of crystal phase-dependent structural changes in the electrode. Simultaneous characterization of the stress and structural changes are achieved concurrently *in situ operando*. The results show excellent agreement with previous literature reports on both phenomena.

1. Introduction

Li-ion battery (LIB) electrodes react with Li ions through an intercalation or alloying mechanism. These mechanisms involve continuous volume expansion/contraction-induced stress and structure/phase changes in LIB electrodes, which lead to gradual deterioration of the battery performance. Therefore, there is a need for real-time monitoring platforms capable of providing simultaneous information on the stress and structural evolutions during battery operation.

Different *in situ* analysis techniques have been utilized in order to understand the mechanical changes in LIB electrodes. Among these, a multi-beam optical sensor (MOS) was shown to be an effective method for characterizing Li-ion battery thin film electrodes [1]. This method enables measurement of important mechanical parameters such as average stress, biaxial modulus and fracture energy for both silicon thin film and commercial electrodes. While the technique has proven to be beneficial for mechanical characterization, limited capability to directly access the electrode hinders its potential integration with other methods for providing structural information.

In parallel, a significant amount of effort has been put into analyzing structural changes in LIB electrodes during battery operation. *In situ* nuclear magnetic resonance (NMR) spectroscopy is used to study detailed kinetics of the electrochemical lithiation and delithiation reactions in nm-sized silicon-based anodes over multiple cycles [2]. Compared to the NMR technique, which relies on bulky

---

* To whom any correspondence should be addressed.

external equipment and complex electrochemical cells, Raman spectroscopy is a valuable tool for analyzing structural and chemical variations in LIB electrodes in a relatively simple fashion. Nevertheless, these methods are restricted to providing only structure or crystal phase (from now on 'phase') evolutions during lithium cycling.

In this work, an *in situ operando* approach is presented, which enables characterization of stress changes using interferometry in parallel with structural changes *via* Raman spectroscopy in a single experiment. The V_2O_5 LIB electrode is used as a model electrode in this work. Additionally, visual observation of phase-dependent asymmetric changes in the electrode is achieved.

2. Design and Fabrication

2.1. Design
The MEMS sensor consists of a Fabry-Perot (FP) cavity and a battery cavity separated by a flexible membrane (figure 1a). The reflective surface of the membrane forms one side of the FP interferometer, while a bonded glass wafer forms the other. The reverse side of the flexible membrane houses a battery cavity coated with the active battery material (V_2O_5). When the battery cavity is exposed to lithium-conducting electrolyte, and metallic Li foil is incorporated as a counter electrode, this device operates a half-cell Li-ion battery. During electrochemical battery operation, the V_2O_5 electrode experiences expansion and contraction as a result of Li-ion insertion/extraction, inducing stress changes in the electrode. These stress changes cause deflection in the flexible membrane (figure 1b), changing the interference patterns accordingly. These pattern changes are recorded and analyzed for stress change characterization. The structure evolutions in the electrode are monitored using Raman spectroscopy which can simultaneously probe the electrode surface through the intervening thin or transparent layers (figure 1b).
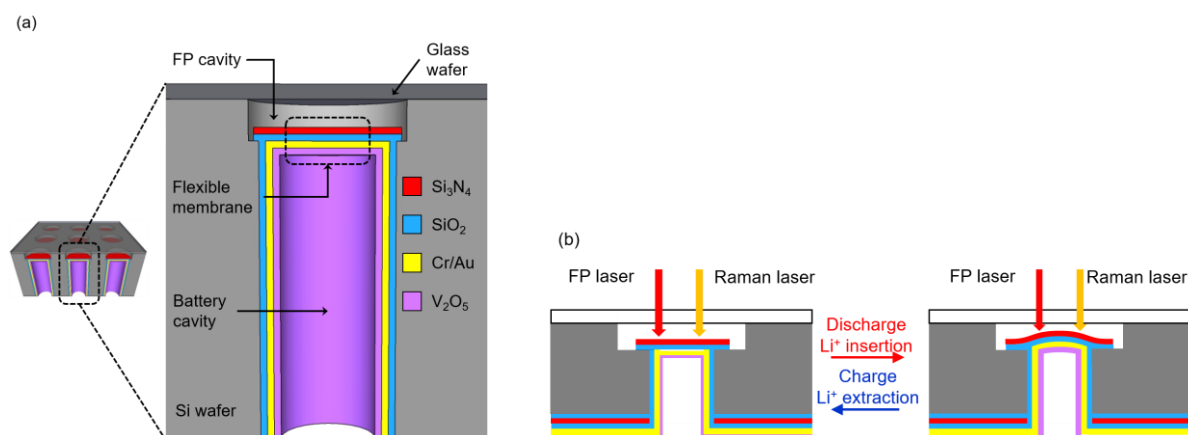

Figure 1. (a) 3D and cross-section schematic of MEMS sensor and (b) schematic representation of the sensing mechanism.

2.2. Fabrication
A double-side polished silicon wafer is used as the substrate for the MEMS sensor fabrication. First, the FP cavity (10 μm deep) is etched using deep reactive-ion etching (DRIE). A 300 nm thick layer of SiO_2 is thermally grown followed by the deposition of a 700 nm thick layer of Si_3N_4 on both sides of the wafer using low pressure chemical vapor deposition. The battery cavity (288 μm deep) is formed by DRIE on the wafer backside, aided by the SiO_2 etch-stop layer. The diameter of the battery cavity (150 μm) determines the diameter of the membrane. A glass wafer is anodically bonded to form the optical FP cavity. The cross-section SEM image (figure 2a) shows well-defined optical and battery cavities separated by the membrane. An additional SiO_2 passivation layer (50 nm) is deposited followed by Cr/Au (5 nm/15 nm) thin films to form the current collector. Finally, the battery cavity is

coated with a thin-film V_2O_5 (135 nm) electrode using atomic layer deposition (ALD) (figure 2b). On finishing the fabrication process, the MEMS sensor device is packaged in a modified coin cell for testing. The complete fabrication process and device packaging are described in detail in our previous work [3].
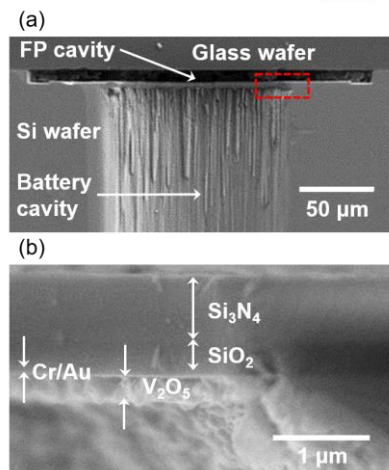

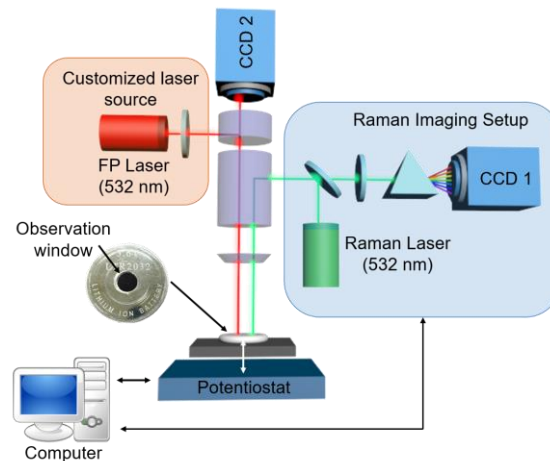**Figure 2.** (a) Cross-section SEM of the membrane and (b) enlarged view highlighting the well-defined multi-layer structure.

Figure 3. Simplified schematic of the experimental setup showing the coin cell under test relative to the Raman microscope.

3. Experimental set-up
A modified coin cell with an optical window is devised to facilitate the experiment during battery operation (figure 3). The assembled coin cell is connected to a potentiostat (Compactstat, Ivium Technologies) and placed under a Raman microscope (Yvon Jobin LabRam Aramis, Horiba, Ltd.) for testing. The white-light illumination source of the Raman microscope is replaced with a customized laser source (532 nm) for measuring the membrane deflection by utilizing the FP interferometry, while the Raman system laser (532 nm) is used as the excitation source for Raman spectroscopy measurements. By employing FP interferometry, the same microscope used for the Raman microspectroscopy analysis can be used to collect information on the membrane deflection, thus enabling multi-modal, real-time monitoring in a unified setup. All these measurements are conducted in air under normal ambient conditions.

4. Results

4.1. Qualitative stress change characterization
Previously, utilizing a similar sensing platform, the stress changes were characterized by monitoring the radius change of one of the concentric rings in the interference patterns [3]. However, the magnitude of the radius change can be quite small when the stress changes in the electrode are not large enough, which can lead to losing subtle or critical stress changes in the electrode. To overcome this limitation, the stress changes in the electrode are characterized instead by analyzing the interference intensity change at the center of the membrane, which is the part of the membrane most sensitive to stress changes. The intensity change induced by the electrode underneath the membrane is calculated based upon the comparison between a pristine electrode and an electrode under electrochemical testing as shown in figure 4a. The correlation between electrochemical data and changes in interference pattern intensity for the membrane during the first electrochemical cycle is shown in figure 4b. Upon lithium insertion (Discharge), the V_2O_5 generally experiences increasing

tensile stress, and the opposite trend is observed during the charge process. Breaking these general trends are two abnormal regions (figure 4b, region I and II), which correspond to elongation/contraction in the lattice constant (*c*) of the crystalline V_2O_5 during the ε- to δ-phase and δ- to ε-phase transformations [4]. These smaller abnormal changes are not detected when the fringe radius monitoring method [3] is applied to the same experimental data used in this work, which demonstrates the enhanced sensitivity of the center intensity monitoring method.
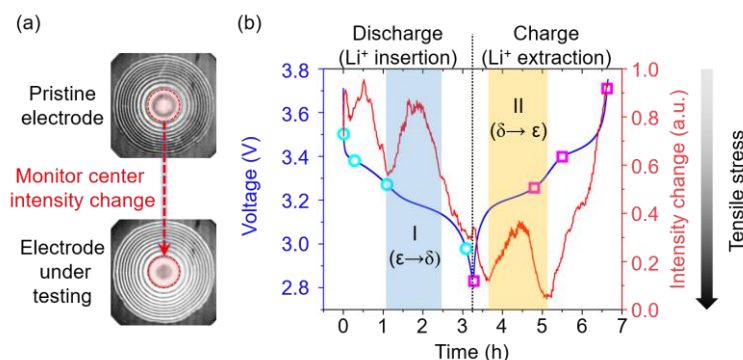

Figure 4. (a) Interference patterns from pristine electrode and electrode under test indicating center intensity change and (b) correlation between the intensity change and discharge-charge curve of the first cycle.

4.2. Structural changes

Simultaneously, *in situ* Raman spectra are collected and representative data at various points along the discharge-charge curve (indicated by blue circles and red squares in figure 4b) are plotted (figure 5). Initially, nine distinct peaks associated with the V_2O_5 electrode are observed. It has been reported that the Raman intensity change at 145 cm^{-1} indicates the level of disorder between V_2O_5 layers [4]. As the level of disorder increases during lithium insertion, the Raman peak intensity at 145 cm^{-1} diminishes and shifts to 155 cm^{-1} (figure 5a). Conversely, during lithium extraction, the Raman peak at 153 cm^{-1} shifts back to 145 cm^{-1} and the intensity of the peak is progressively recovered (figure 5b), indicating the V_2O_5 lattice is fully restored. Progressive decrease and full recovery in the intensity of the other eight peaks, as well as the Raman shift at 996 cm^{-1}, verify the high electrochemical reversibility of the electrode [4].
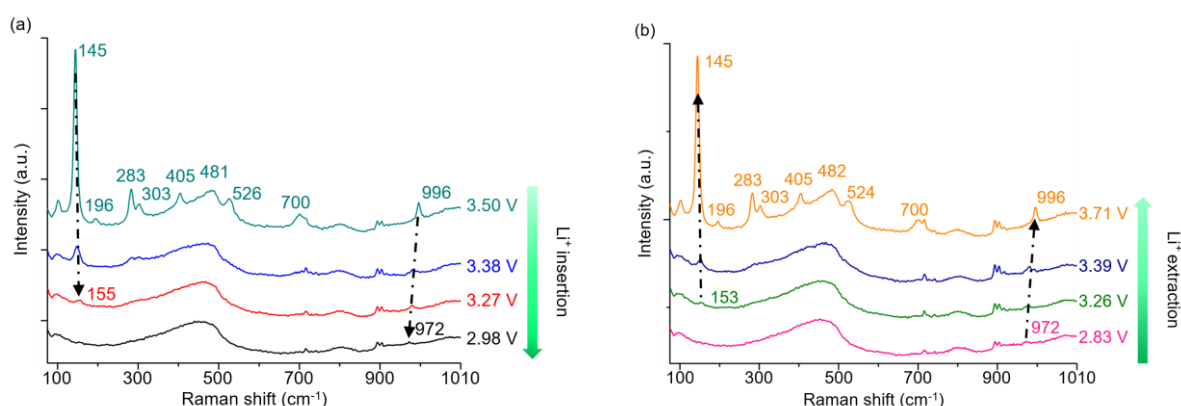

Figure 5. (a) *In situ* Raman spectra collected during first discharge (cyan circles in Figure 5(b)) and (b) charge (magenta rectangles in Figure 5(b)) cycle.

4.3. Visual observation

Visual observation of phase dependent structural changes has a distinct advantage compared to other characterization methods since it allows monitoring of significant structural evolutions in the electrode by merely observing the series of interference pattern images recorded during the experiment. The visual observation of the crystal phase-dependent structural changes in the electrode is shown in figure 6. The interference patterns remain symmetric in the first discharge-charge cycle (figure 6a, region A corresponding to figure 4b), which are the expected interference patterns from a symmetric circular membrane. However, operating over a larger voltage regime in the second cycle, more drastic phase changes can be indirectly visualized through the asymmetric interference patterns themselves (region B), which then reversibly transition back to symmetric patterns (region C) depending on the phase transitions in the V_2O_5 electrode [4].
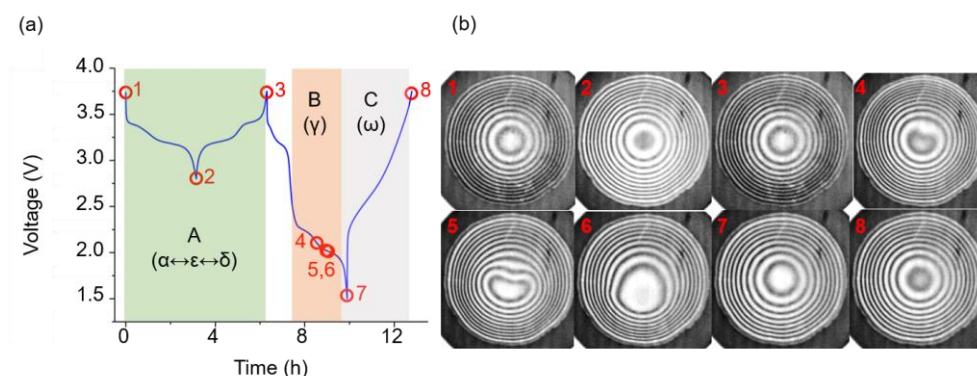

Figure 6. (a) Discharge-charge cycles annotated with the relevant V_2O_5 phase transitions and (b) series of interference images of the circular membrane collected along the discharge-charge curve.

5. Summary
The work presented here demonstrates the capability of the *in situ operando* approach for characterization of LIB electrodes. Stress changes in V_2O_5 electrodes are characterized by monitoring the center intensity changes of the interferometric patterns, yielding higher sensitivity compared to the previously reported method. At the same time, reversible structure changes in the V_2O_5 electrodes are observed by the Raman spectroscopy measurements. These stress and structural evolutions are monitored simultaneously in a unified set-up enabled by the MEMS sensor. Thus, this MEMS platform facilitates simultaneous investigation of electrochemically-driven stress and structural changes in LIB electrodes, and can be leveraged as a discovery platform for various thin-film electrode materials in the field of battery electrode characterization.

6. References
[1]   Sethuraman V A, Chon M J, Shimshak M, Srinivasan V and Guduru P R 2010 *J. Power Sources* **195** 5062-5066
[2]   Ogata K, Salager E, Kerr C J, Fraser A E, Ducati C and Morris 2014 *Nat. Commun.* **5** 3217 (11pp)
[3]   Pomerantseva E, Jung H, Gnerlich M, Baron S, Gerasopoulos K and Ghodssi R 2013 *J Micromech Microeng* **23** 114018 (10pp)
[4]   Baddour-Hadjean R and Pereira-Ramos J –P 2010 *Chem. Rev.* **110** 1278-1319